

Effect of Design and Operating Parameters on the Spray Characteristics of an Outward Opening Injector

Sudhakar Das and Paul G. VanBrocklin

Delphi Corporation
Technical Center Rochester
Rochester, New York

ABSTRACT

Simulation of an outward opening injector using the modified KIVA-3V computational code is reported in this study. Initially, the modified injection model has been validated using the experimental data generated in the laboratory. The effect of computational grid resolution is also reported.

Using the validated code, a parametric study of the effect of *nozzle exit diameter*, *tangential velocity* at the nozzle exit and *streamwise velocity* on the injector characteristics such as spray penetration, Sauter Mean Diameter (*SMD*), and volume distribution (*DV90*) has been carried out. A strong effect of the tangential component of velocity (swirl) at the nozzle exit was observed on the scattering (spread) of spray droplets. The effect of streamwise velocity was comparatively less on the droplet scattering. With a smaller nozzle exit diameter, a large interaction between the vortices formed at the tip of the spray was observed. This is due to proximity between the two counter rotating vortices. Further, the interaction between the vortices are enhanced with increased exit velocities and sometimes resulted in deterioration of spray quality.

1. Introduction

The potential of direct injection gasoline (DIG) engine for improvement of fuel economy and reduction of tailpipe emissions has been well demonstrated by engine researchers [1-5]. This has generated more interest in understanding the complex nature of fuel injection process in next generation DIG systems. Further, the fuel injection requirement for a DIG engine environment is more critical than its port-fuel counterpart as the time available for mixture preparation is much shorter in this case. Being able to run over a wide range of operating conditions, i.e. running in homogeneous mode to stratified charge mode places stringent requirements on DIG fuel

systems. This has lead to the wide spread use of high-pressure injectors able to produce very small droplets within a small CA window. At the same time, these injectors must exhibit very low spray penetration. Despite significant advantage in DIG injector designs, a high variation in the spray characteristics are observed for small changes in the design and operating conditions. It is, therefore, necessary to understand the injector behavior for proper functioning at different operating conditions.

In recent years, mathematical models have been useful tools for shortening the lead-time in the design and optimization process of various automotive components. Computational Fluid Dynamics (CFD) has been used to optimize combustion chamber design investigating incylinder flow effects in combustion characteristics and to study the effect of engine design and operating variables on engine performance [6]. CFD simulations also provide insight of fluid dynamics of fuel spray, and its interaction with the incylinder charge motion [7,8]. Modeling the intricate details of spray atomization process is a very difficult task. It is a common practice to specify velocity at the nozzle exit and initial droplet distribution. Velocity data can be produced using the steady state flow through the nozzle, whereas, the droplet distribution data are typically obtained from experiment. All simple atomization models such as the Taylor Analogy Breakup (TAB), Kelvin-Helmholtz (K-H) wave and Rayleigh-Taylor (R-T) instability [9-11] require some tuning of constants based on the injector geometry and operating conditions.

In the present study, the TAB model has been used with some modification for the atomization process. At the nozzle exit, both tangential and streamwise velocities are prescribed and these velocities are dependent on operating pressures (both upstream and downstream pressure conditions). Parametric studies were carried out with varying nozzle exit diameter, exit velocity components at the

nozzle tip and pintle seat angles. The spray characteristics measured are (a) spray penetration (b) Sauter Mean diameter (c) spray droplet distribution (DV50, DV90 etc) and (d) spray cone angle (spray collapse). The spray collapsing criteria is described in the later section.

2. Mathematical Model

2.1 Outward Opening Injection Spray Model

The existing Taylor Analogy Breakup (TAB) atomization model in KIVA-3V code was used for atomization (droplet breakup). The basic structure of the code is for spray originating from an orifice. The simulation of an outwardly opening injector necessitated modification in the existing spray model. These modifications are listed below:

Initially, the spray droplet was assigned a position at the axis of the nozzle at the tip level. A random number generator was used to assign this droplet randomly around the annulus of the pintle diameter and seat as shown in Figure 1. Instantaneous droplet position is given by:

$$(d_0/2) \cdot 2 \cdot \pi \cdot \text{Rand}(0) \quad \dots[1]$$

where, d_0 is the pintle diameter and $\text{Rand}(0)$ is the random number generator function

The liquid film sheet was not modeled because of the complexity involved in this type of modeling. The initial droplet diameter is based on the instantaneous lift of the pintle.

$$d_b = l \sin \theta \quad \dots[2]$$

where, d_b is the initial blob diameter used in the breakup calculation, l is the instantaneous pintle lift, and θ is the half seat angle.

The instantaneous flow area is calculated using the relation

$$a_0 = \pi \cdot (d_0 + l \sin \theta \cdot \cos \theta) l \sin \theta \quad \dots[3]$$

where, a_0 is the nozzle exit area and d_0 is the pintle diameter

Normal and tangential velocity components were specified for the swirling motion at the nozzle exit.

The amplitude oscillation factor, $amp0$ used in the TAB model is based on diesel injector models. As the initial velocity of a spray emerging from a DIG injector nozzle will be considerably different from that of a diesel injector, the validity of such a model applied to DI-G injection process is always questionable. The magnitude of $amp0$ in a DI-G injector could be significantly different than in the case of a diesel injector due to the order of magnitude difference in their injection velocities. Thus, the subjectivity of this parameter was eliminated by using

an $amp0$ value based on the pintle stroke as suggested by Dan *et al* [12]. The $amp0$ values at varying stroke of the pintle were computed using the following equation:

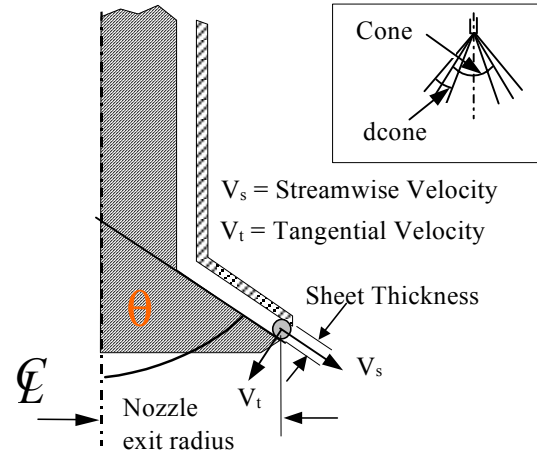


Figure 1. Schematic diagram of the injection model

$$amp0 = \frac{1}{c_b r_0 \omega_0} \cdot \sqrt{\frac{2}{3}} k_0 \quad \dots[4]$$

where, c_b , r_0 , and ω_0 are constants determined by the input value and properties of the injected fuel. k_0 is the turbulent kinetic energy for liquid flow at nozzle exit.

Initial frequency of droplet oscillation was computed using the equation [12]:

$$\omega_o = \sqrt{C_k \frac{\sigma}{\rho_l r_o^3} - \left(\frac{C_d \mu_l}{2 \rho_l r_o^2} \right)^2} \quad \dots[5]$$

where, $C_k (=8.0)$, $C_b (=0.5)$, $C_d (=5.0)$ are constants and ρ_l , μ_l , σ and r_o are respectively the density, viscosity, surface tension and radius of the liquid droplet. Here, r_o is based on the instantaneous pintle position.

The initial turbulent kinetic energy was set equal to 10 percent of the mean flow energy based on the instantaneous value of droplet velocity, V_{inj} .

Finally, variations in both the nozzle exit area (stroke) and velocity during the injection process were assigned using the measured pintle motion information. The average flow velocity at each point in the pintle lift curve was calculated using steady state flow bench information with the stroke set at discrete values, coupled with the corresponding nozzle exit area values.

3. Computational Domain

In this study, a cylindrical domain with a 105 mm diameter and 308 mm height has been used to simulate pressure chamber conditions. Figure 2 shows the computational grid used to represent the computational domain with approximately 325,000 cells. The injector seat area was modeled as close to the actual geometry as possible to capture the salient features.

The normal and tangential velocities at the nozzle exit were computed using the steady state flow simulation with Fluent6.0 CFD code. This data was used as input to the KIVA-3V code for spray atomization.

In the simulation, the gasoline fuel was injected into air with an initial temperature corresponding to the adiabatic compression temperature at the chamber pressure.

4. Method used for Analysis of Simulation Data

4.1 Injection Characteristics

Simulation data was analyzed based on the experimental setup and analysis method used in the spray laboratory. Droplet properties such as penetration, Sauter Mean Diameter (SMD), droplet number distribution and volume distribution were used for comparison with experimental data.

In the spray laboratory, an imaging technique is used to measure spray penetration. Laser Doppler Anemometry (LDA) is used to characterize the droplet properties such as Sauter Mean Diameter (SMD), DV90 etc. The laser beam used has a 15 mm diameter and the centerline is at a distance of 30 mm from the tip of the nozzle. A schematic is shown in Figure 3.

Spray penetration at a given time is computed as the distance from the tip of the nozzle that includes 95% of the injected volume. This will avoid overestimation of spray penetration affected by stray droplets in the domain.

4.2 Criteria for Spray Collapse

The width of the spray and the spray cone angle were measured at a distance from the tip of the nozzle using the droplet images from the simulation. Finally, using this spray cone angle at two different chamber pressures, the spray collapse is calculated. A collapse number is the ratio of change in spray angle (SA) to its nominal angle (injector seat angle) when the injector is run at two different chamber pressures (P1 and P2). The average value is calculated over a period of time.

$$\text{Collapse Number} = \frac{SA_{P1} - SA_{P2}}{\text{SeatAngle}}$$

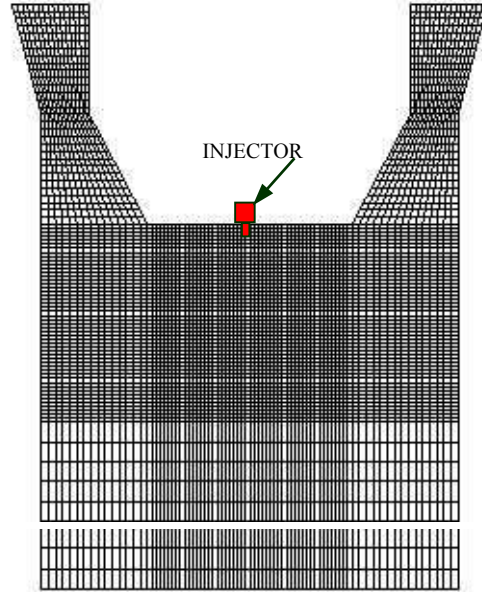


Figure 2. Computational domain and grid used in the simulation study

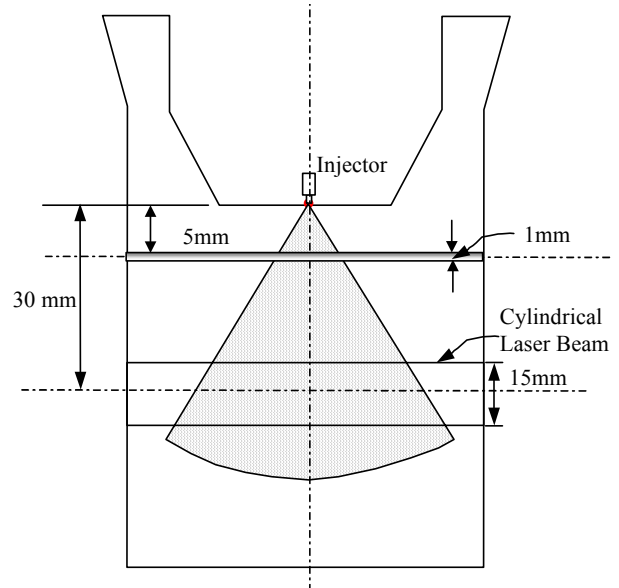


Figure 3. Schematic diagram showing the LDA data simulation and spray width measurement at 5 mm from the tip of the nozzle

5. Validation of Computational Model

Initial model validation was carried out for a mesh size of 210,000 cells. Test parameters for spray penetration, SMD and DV90 simulation results are given in Table 1. Experimental data for this matrix was also obtained for comparison.

In most cases, 20MPa injection pressure and 10,000 parcels of spray droplets were used for injection simulation. Otherwise, any deviation from the above simulation conditions has been mentioned with the results.

Table 1. Simulation Matrix

Seat Angle	Chamber Pressure, bar	Tem °C	Velocities, m/s	
			Swirl	Streamwise
60	1	25	68.06	55.99
	4.0	150	67.64	55.57
	11.7	302	65.94	54.44
80	1	25	65.05	54.82
	4.0	150	64.75	54.41
	11.7	302	63.30	53.32

Figure 4 shows the comparison between simulated and measured spray penetration for 60-degree seat angle at 1bar ambient pressure. The spray penetration in the early stage is well simulated using the CFD model, however, there is some deviation observed in the later time. This may be attributed to the thickness of the hollow cone spray. In this simulation, a *d*cone value of 11 degree has been used based on the data for a 10MPa outwardly opening injector. Other factors such as machining tolerances and surface finish aspects that are not represented in the model can also have an effect. Nevertheless, the model predicts the trend within an accuracy of 10 percent in the region of interest, usually up to 1 ms after the start of injection. This is within a reasonable limit to be used to extract the spray characteristics of the outwardly opening injector.

Time averaged Sauter Mean Diameter and DV90 data have been compared in Figure 5. The numbers in parentheses represent the seat angle of the pintle. The simulated results compare well with the measured data except for the DV90 values in the case of 80-degree seat angle. It appears that the spread of droplets are responsible for this discrepancy. As with the case of 80-degree seat angle, the spray droplets tend to move further away from the axis of the injector. The scattering of a droplet will be more in this case resulting in the deviation between simulated and measured data.

6. Effect of Grid Resolution on Simulation Results

The effect of grid resolution has always been questionable for any simulation work as sometimes the quality of grid (i.e. aspect ratio, skewness/warpage) significantly affects the computational results. In general, the amount of numerical diffusion

is inversely proportional to the grid resolution. Numerical diffusion can also be minimized by aligning the mesh along the flow direction [13]. Mesh refinement invariably increases the computational expense and hence drives the need for an optimum grid resolution that results in acceptable accuracy.

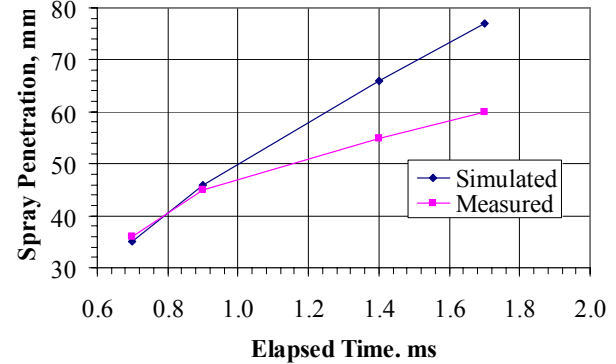


Figure 4. Comparison between simulated and measured spray penetration

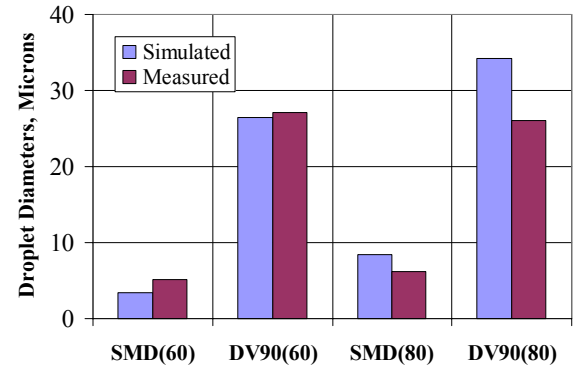


Figure 5. Comparison between simulated and measured SMD and DV90 at 1bar chamber pressure

In this study, the effect of mesh resolution was studied with a 60° seat injector using mesh sizes of 210,000 cells and 325,000 cells. A maximum number of 50,000 droplet parcels used in the simulation. The results obtained are given in Table-2.

As seen from Table 2, there is no significant difference observed in the spray characteristics such as spray penetration, SMD and DV90 values at various pressures for the two mesh resolutions considered in this study. This further supports that the model results are repeatable within acceptable limits.

Further, the mesh resolution was increased to 780,000 cells. With this very fine resolution, both the SMD as well as DV90 values were found to increase. This may be the result of a flooding of droplets in the computational cell and requires more study using increased number of droplet parcels to understand this deviation.

Table 2. Effect of Mesh Resolution on Spray Results (60 Deg Seat Angle, 50,000 droplet parcels)

Pressure bar	Number of Cells	Penetration [†] mm	SMD [†] μm	DV90 [†] μm
1.0	210,000	38.57	4.9	30
	325,000	37.43	6.12	36
4.0	210,000	26.51	18.69	44
	325,000	26.70	21.56	46.0
11.7	210,000	20.35	18.31	40.0
	325,000	19.45	20.66	38.0

[†] Values at 0.8ms after start of injection

7. Parametric Studies-Results and Discussions

7.1 Effect of Seat Angle (60° versus 80°)

With some hardware designs cone collapse can be observed. The collapsing cone may be attributed to the interaction between two counter-rotating vortices. For a particular injector design series, spray with a 60° seat angle was observed to have collapsing tendencies when compared to its 80° counterpart. Figure 6 shows that for the 80° seat angle case, the two counter-rotating vortices are far apart from each other avoiding significant interaction. The spray characteristics such as SMD, DV90 were however found very close to that of the 60° seat angle case.

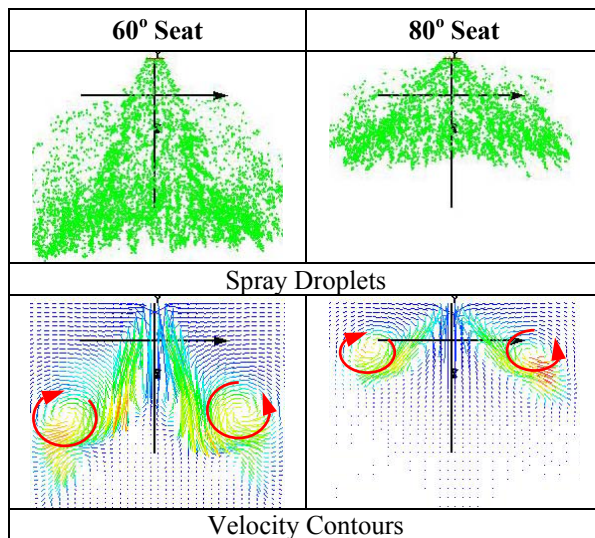


Figure 6. Spray Droplets and velocity contours at 1ms after injection (4bar chamber pressure)

7.2 Effect of Swirl Velocity

The effect of swirl velocity on injection characteristics was studied keeping the momentum of the spray constant, i.e. the resultant velocity at the exit kept constant. In the no swirl case, the effective streamwise velocity is therefore more than the swirling velocity case to match the momentum.

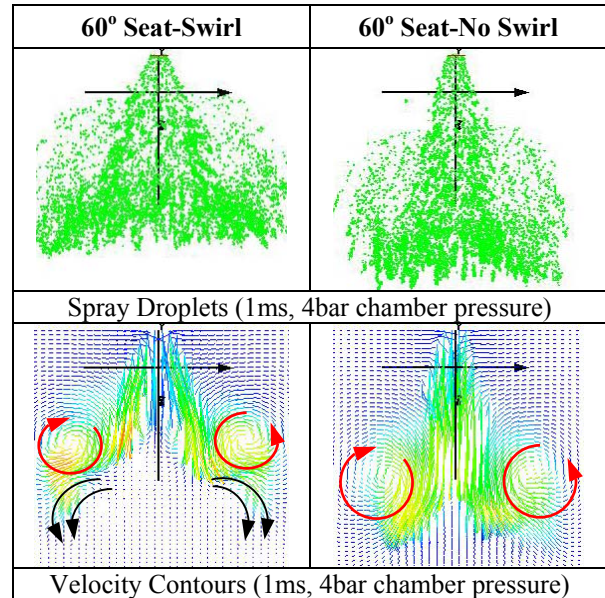


Figure 7. Comparison of spray droplets and velocity contours (swirl versus no swirl case)

There was no significant difference observed in SMD and DV90 values for the swirl and no swirl cases, however, the spray penetration was considerably higher in no swirl case. This corresponds to the practical aspect of inducing swirl to reduce penetration without compromising other spray characteristics. With the no-swirl case, the distance between the centers of two counter-rotating vortices are increased. This helps reduce the interaction between the two vortices – a primary cause for collapsing spray.

7.3 Effect of Streamwise velocity

The effect of varying streamwise velocity was studied for a chamber pressure of 4bar. The tangential component was kept constant at 68m/s and the streamwise component of velocity was varied from 55 to 80 and 120m/s. The velocity plots are shown in Figure 8.

With an increase in streamwise velocity, spray penetration (shown as numbers in Figure 8) was also increased, however, the SMD and DV90 values remained constant.

7.4 Effect of Nozzle Exit diameter

The effect of nozzle exit was studied using exit diameters of 2mm (baseline), 3mm and 4mm. The flow rate was kept constant for all the three cases. As the flow area increased, the velocity components at the nozzle exit were reduced proportionately. The spray characteristics deteriorated considerably with increased nozzle exit diameter. With the increased exit diameter, the distance between the two counter-rotating vortices were also increased resulting in reduction of spray collapse.

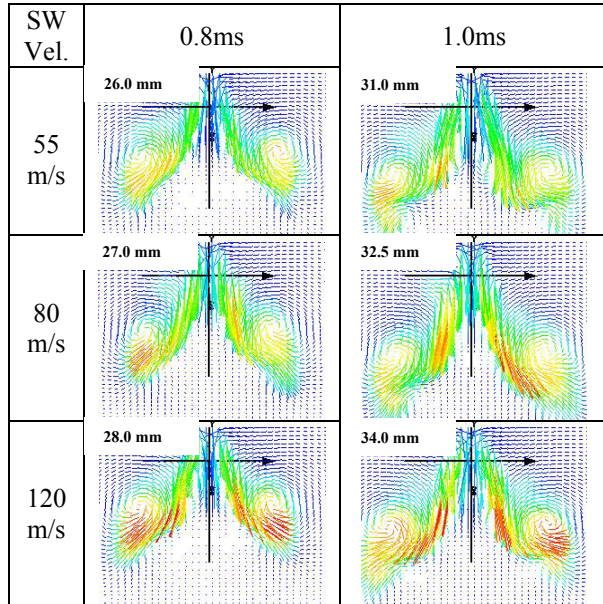


Figure 8. Effect of streamwise velocity on spray (4bar chamber pressure)

8. Conclusions and Recommendations

This study shows that computational models can be used to understand some basic issues related to the performance of a DI-G injector.

Based on the simulation study, collapsing spray can be influenced by the following:

- Seat angle
- Streamwise velocity/tangential velocity
- Nozzle exit diameter

The above design and operating parameters must be optimized to obtain an acceptable spray quality for a particular use of DIG injector.

ACKNOWLEDGMENTS

The authors would like to thank G. Geiger and E. Suh, N. Mastro of Delphi's Technical Center Rochester and D. Robart, B. Befrui of Delphi's Technical Center Luxembourg for their valuable suggestions.

REFERENCES

1. Zhao, F., Lai, M-C, and Harrington, D. L., *Automotive Spark Ignited Direct-Injection Gasoline Engine, Progress in Energy and Combustion Science (JPECS)*, Vol.25, No. 5, pp.437-562, 1999.
2. Kume, T., Iwamoto, Iida, K., Murakami, M. Akishino, K, and Ando, H., *Combustion Control Technologies for Direct Injection SI Engine*, SAE Paper 960600, 1996.
3. Spiegel, L. and Spicher, U., *Mixture Formation and Combustion in a Spark Ignition Engine with Direct Fuel Injection*, SAE Paper No. 920521, 1992.
4. Preussner, C., Döring, C., Fehler, S. and Kampmann, S., *GDI: Interaction Between Mixture Preparation, Combustion System and Injector Performance*, SAE Paper 980498, 1998.
5. Fraidl, G. K., Piock, W. F. and Wirth, M., *Gasoline Direct Injection: Actual Trends and Future Strategies for Injection and Combustion Systems*, SAE Paper 960465, 1996
6. Das, S., Houtz, P. J., and Reitz, R. D., *Effect Of Injection Spray Angle And Combustion Chamber Geometry On Engine Performance And Emission Characteristics Of A Large Bore Diesel Engine*, ASME Paper No. 99-ICE-159 ICE-Vol. 32-1, 1999 Spring Technical Conference.
7. Kneer, R, Befrui, B, Weiten, C, Adomeit, P, Geiger, J Ballauf, J and Voft, B, *Close-Arranged Spray-Guided DISI: Application of a High Pressure Outward-Opening Injector*, Spaper presented at 11 Aachen Colloquia, 2002.
8. VanDerWege, B.A., Lounsberry, T.H., and Hochgreb, S, *Numerical Modeling of Fuel Sprays in DISI Engines Under Early-Injection Operating Condition*, SAE Paper 2000-01-0273, 2000.
9. O'Rourke, P. J., and Amsden, A.A., *The TAB Method for Numerical Calculation of Spray Droplet Break-up*, Paper 872089, 1987 (TAB)
10. Chan, M., Das, S and Reitz, R.D., *Modeling Multiple Injection and EGR Effects on Diesel Engine Emissions*, SAE Paper 972864,1997.
11. Allocca, L., Bella, G., De Vita, A., and DI Angelo, L, *Experimental Validation of a GDI Spray Model*, SAE Paper 2002-01-1137, 2002.
12. Dan, T. and Lai, M. C., *Modeling of Turbulent Primary Breakup in Diesel Spray*, 11th Annual Conference on Liquid Atomization and Spray Systems (ILASS), Sacramento, CA, May 1998.
13. Fluent 6.0 Users Manual